Dispersive waves emitted by solitons perturbed by third-order dispersion inside optical fibers

Samudra Roy,[1] S. K. Bhadra,[1] and Govind P. Agrawal[2]

[1]*Central Glass and Ceramic Research Institute, CSIR, 196 Raja S. C. Mullick Road, Kolkata-700032, India*
[2]*Institute of Optics, University of Rochester, Rochester, New York 14627, USA*

Solitons forming inside optical fibers are perturbed by several higher-order dispersive and nonlinear effects, especially when ultrashort optical pulses are used to excite them. We study, both analytically and numerically, how the radiation emitted by solitons in the form of dispersive waves (sometimes called Cherenkov radiation) is affected by these higher-order effects. Our results show that a certain minimum amount of third-order dispersion is needed before the amplitude of the dispersive wave becomes large enough for a spectral peak to appear in the output spectrum. This minimum value depends on the soliton order N and decreases with increasing N. The amplitude of the radiation peak increases initially with both the magnitude of the third-order dispersion and the soliton order, but then saturates to a relative power level that is typically below 10% of the launched power. Our results reveal several interesting features that should be of relevance for applications requiring an ultrabroadband optical source.

I. INTRODUCTION

It is well known that ultrashort pulses can propagate as optical solitons in the anomalous-dispersion region of an optical fiber [1–4]. However, such solitons are perturbed by several higher-order dispersive and nonlinear effects, especially when ultrashort optical pulses are used to excite them. Such perturbations, although undesirable for some applications, also lead to interesting phenomena such as soliton fission [5], intrapulse Raman scattering (IPRS) [6], dispersive-wave radiation [7], and supercontinuum generation [8]. Among these, the emission of nonsolitonic radiation (NSR) in the form of dispersive waves (also called Cherenkov radiation) is of particular importance for supercontinuum generation [9–12]. It was first identified in 1986 in numerical simulations [7] and studied in considerable detail [13–18] during the 1990s for the specific case in which a fundamental soliton is perturbed by third-order dispersion (TOD) alone.

In practice, optical pulses are often propagated as higher-order solitons, which are perturbed by several other nonlinear effects, such as IPRS and self-steepening, as they propagate down the fiber. Our objective in this study is twofold. First, we extend the analysis of Akhmediev and Karlsson [17] and find different analytic expressions for the frequency and amplitude of the NSR peak that is generated in the output spectrum when a higher-order soliton is perturbed by the TOD. Second, we perform extensive numerical simulations to test how well this analytic prediction holds under more realistic conditions in which the soliton is also affected by higher-order nonlinear effects such as IPRS and self-steepening. Our results reveal several interesting features that should be of relevance for applications in which a supercontinuum source is required.

The paper is organized as follows. We review in Sec. II the earlier work and extend it to derive modified analytic expressions for the NSR frequency and amplitude. The numerical results based on the generalized Schrödinger equation (NLSE) are presented in Sec. III. They are then used in Sec. IV to study the evolution of the NSR frequency and amplitude with the strength of TOD. Section V focuses on how these two quantities vary with the order of the soliton (or the launched peak power). The main results are then summarized in Sec. VI.

II. NSR FREQUENCY AND AMPLITUDE

We begin by reviewing briefly the analytic results of Akhmediev and Karlsson [17]. If we include only the TOD perturbation, the NLSE has the following normalized form:

$$i\frac{\partial U}{\partial \xi} - \frac{\text{sgn}(\beta_2)}{2}\frac{\partial^2 U}{\partial \tau^2} + N^2|U|^2 U = i\delta_3\frac{\partial^3 U}{\partial \tau^3}, \qquad (1)$$

where the field amplitude $U(\xi,\tau)$ is normalized such that $U(0,0)=1$ and the other dimensionless variables are defined as [4]

$$\xi = \frac{z}{L_D}, \quad \tau = \frac{t - z/v_g}{T_0}, \quad N = \sqrt{\gamma P_0 L_D}, \quad \delta_3 = \frac{\beta_3}{6|\beta_2|T_0}. \qquad (2)$$

Here, T_0 and P_0 are related to the width and the peak power of the ultrashort pulse launched into the fiber, $L_D = T_0^2/|\beta_2|$ is the dispersion length, v_g is the group velocity, γ is a nonlinear parameter, β_2 is the second-order dispersion parameter, and β_3 is the TOD parameter of the fiber. The dimensionless quantity N is the soliton order defined such that $N=1$ for a fundamental soliton [4]. In the absence of TOD ($\delta_3 = 0$) and the presence of anomalous dispersion ($\beta_2 < 0$), Eq. (1) predicts that, when $N=1$, an input pulse with the amplitude $U(0,\tau) = \text{sech}(\tau)$ propagates as the fundamental soliton with the general solution $U(\xi,\tau) = \text{sech}(\tau)\exp(i\xi/2)$. Clearly, such an input pulse maintains its shape and width perfectly. This scenario ceases to occur when the fundamental soliton is perturbed by the TOD ($\delta_3 \neq 0$).

It turns out that a TOD perturbation manifests through emission of NSR at a frequency different from those associated with the soliton [13]. Normally, a dispersive wave can-

not be phase matched with a fundamental soliton whose wave number lies in a range forbidden for a linear dispersive wave. However, the presence of TOD can lead a phase-matched situation in which energy is transferred from the soliton to the dispersive wave at a specific frequency. In our notation, this frequency is given by a relatively simple expression [17],

$$\Delta\nu_d T_0 \approx \frac{(1+4\delta_3^2)}{4\pi\delta_3}, \tag{3}$$

where $\Delta\nu_d = \nu_d - \nu_s$, and ν_s and ν_d are the carrier frequencies associated with the soliton and the dispersive wave, respectively. It is also possible to calculate the peak power level P_d of the NSR, and the perturbative result, correct to first order in δ_3, is given by [17]

$$p_d = \frac{P_d}{P_0} \approx \left(\frac{5\pi}{4\delta_3}\right)^2 \left(1-\frac{2\pi}{5}\delta_3\right)^2 \exp\left(-\frac{\pi}{2\delta_3}\right). \tag{4}$$

One may ask whether Eqs. (3) and (4) apply when the input pulse propagates as a higher-order soliton, the situation encountered commonly for supercontinuum generation. In this case, the TOD and IPRS induce the fission of the higher-order soliton such that the Nth-order soliton splits into N fundamental solitons of different widths and amplitudes [5,7]. The most energetic soliton has a width T_s that is $(2N-1)$ times smaller than the input pulse width T_0 and its peak power is larger by a factor of $(2N-1)^2/N^2$ [4]. The theory of Ref. [17] should be applied to this soliton because it is perturbed the most by TOD. The frequency and the amplitude of the dispersive wave can again be obtained using the same procedure, and the result is found to be

$$\Delta\nu_d T_0 \approx \frac{1}{4\pi\delta_3}[1+4\delta_3^2(2N-1)^2], \tag{5}$$

$$p_d \approx \left(\frac{5\pi N}{4\delta_3}\right)^2 \left(1-\frac{2\pi}{5}(2N-1)\delta_3\right)^2 \exp\left(-\frac{\pi}{2(2N-1)\delta_3}\right). \tag{6}$$

It should be stressed that the preceding expressions apply only for the shortest soliton (with maximum peak power), which is primarily responsible in generating NSR. Other solitons also produce dispersive waves but their amplitudes remain relatively low. Figure 1 shows how the NSR power p_d varies (a) with δ_3 for a fixed N and (b) with N for a fixed δ_3, using the analytical result given in Eq. (6). In both cases, we assume that a relative power level of 10^{-8} (or -80 dB) is the lowest limit for the formation of the NSR peak in the output spectrum. We note that a minimum value of δ_3 is needed before the onset of the NSR but this value depends strongly on the soliton order N. For example, δ_3 should exceed 0.06 for $N=1$ but this value is reduced to below 0.02 for $N=2$. Once the NSR peak has formed, its amplitude grows rather rapidly with both δ_3 and N because of the exponential term in Eq. (6). We should also stress that the validity of Eq. (6) becomes doubtful once the relative power of the NSR has reached a level close to -15 dB because of a perturbative approach requiring $(2N-1)\delta_3 \ll 1$ used to derive it.
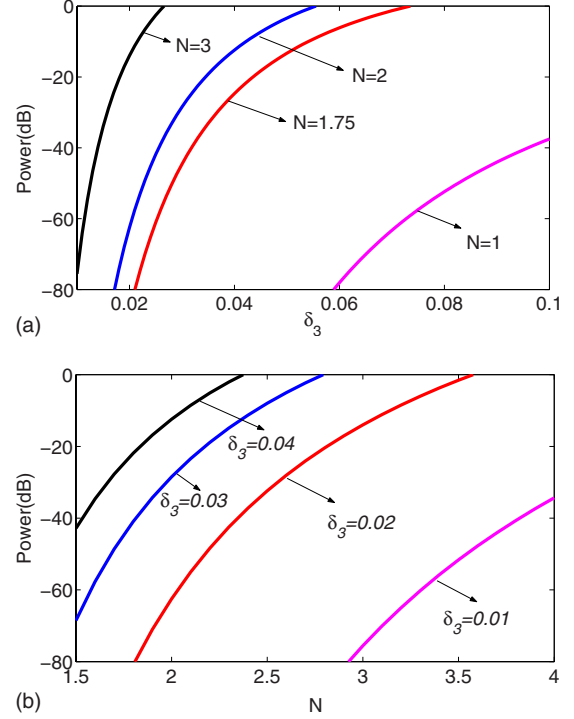
FIG. 1. (Color online) Variation of NSR power (a) with the TOD parameter δ_3 and (b) with the soliton order N based on the analytic result in Eq. (6).

III. IMPACT OF HIGHER-ORDER NONLINEAR EFFECTS

The preceding result holds when a higher-order soliton is perturbed by the TOD alone. In practice, such a soliton is also influenced simultaneously by two other higher-order nonlinear effects, namely, IPRS and self-steepening. Clearly, the NSR would also be affected by them. To study their impact on NSR, we assume $\beta_2 < 0$ and use the generalized NLSE in the following normalized form [4]:

$$\frac{\partial U}{\partial \xi} = \frac{i}{2}\frac{\partial^2 U}{\partial \tau^2} + \delta_3\frac{\partial^3 U}{\partial \tau^3} + iN^2\left(1+is\frac{\partial}{\partial \tau}\right)$$
$$\times\left(U(\xi,\tau)\int_{-\infty}^{\tau} R(\tau-\tau')|U(\xi,\tau')|^2 d\tau'\right). \tag{7}$$

Here, $s = (2\pi\nu_s T_0)^{-1}$ is the self-steepening parameter and $R(\tau)$ is a nonlinear response function of the optical fiber in the form

$$R(\tau) = (1-f_R)\delta(\tau) + f_R h_R(\tau), \tag{8}$$

where $f_R = 0.245$ and the first and the second terms correspond to the electronic and Raman responses, respectively. As discussed in Ref. [19], the Raman response function can be expressed in the form

$$h_R(\tau) = (f_a + f_c)h_a(\tau) + f_b h_b(\tau), \tag{9}$$

where the functions $h_a(\tau)$ and $h_b(\tau)$ are defined as

$$h_a(\tau) = \frac{\tau_1^2 + \tau_2^2}{\tau_1 \tau_2^2}\exp\left(-\frac{\tau}{\tau_2}\right)\sin\left(\frac{\tau}{\tau_1}\right), \tag{10}$$

$$h_b(\tau) = \left(\frac{2\tau_b - \tau}{\tau_b^2}\right)\exp\left(-\frac{\tau}{\tau_b}\right),$$

and the coefficients $f_a=0.75$, $f_b=0.21$, and $f_c=0.04$ quantify the relative contributions of the isotropic and anisotropic parts of the Raman response. In Eq. (10), τ_1, τ_2, and τ_b have values of 12, 32, and 96 fs, respectively. In our notation, they have been normalized by the input pulse width T_0.

We employ the standard split-step Fourier method [4] to solve Eqs. (1) and (7) numerically for values of δ_3 in the range of 0 to 0.1. The input "sech" pulses are assumed to have a carrier wavelength of 835 nm and a width such that $T_0=50$ fs (full width at half maximum of about 88 fs). Their peak power is varied such that the soliton order N varies from 1 to 4. In the following simulations, the fiber length corresponds to four dispersion lengths (ξ varies from 0 to 4). The physical fiber length depends on the value of β_2 and would be 10 m for $\beta_2=-1$ ps^2/km. We stress that the self-steepening effects are negligible in our simulations because $s<0.01$ for $T_0=50$ fs. Thus, IPRS is the major higher-order nonlinear process affecting the numerical simulations performed by varying δ_3 in the range of 0 to 0.1. Note that δ_3 can take negative values if the TOD parameter $\beta_3<0$ at the operating wavelength. Since $\nu_d<\nu_s$ in that case, the NSR wavelength falls on the red side of the soliton spectrum. In the following discussion we consider only positive values of δ_3 (blueshifted NSR), but the main conclusions should hold even for negative values of δ_3.

When a fundamental soliton is launched at the input end of the fiber ($N=1$), a peak, indicative of NSR, is generated on the blue side of the pulse spectrum, but its amplitude remains negligible until δ_3 exceeds 0.06. Moreover, the relative power of the NSR peak remains relatively small even for larger values of δ_3. The peak position shifts toward the main central peak with increasing δ_3. All of these features are in agreement with the analytical results shown in Fig. 1 for N =1.

We next focus on the case of higher-order solitons. The gray (red) curves in Fig. 2 show the pulse spectra at $\xi=4$ for four values of δ_3 when a second-order soliton ($N=2$) is launched inside the fiber. The darker (blue) curves show for comparison the spectra obtained when Eq. (1) is employed instead of Eq. (7) so that the IPRS and self-steepening effects are absent. In both cases, the second-order soliton undergoes fission near $\xi=0.5$ but the subsequent evolution is quite different. The case $\delta_3=0$ shown in Fig. 2(a) reveals that the spectrum, broadened by self-phase-modulation, is perfectly symmetric in the absence of IPRS. The impact of IPRS is to produce a redshift of the shortest soliton with the width T_s =$T_0/3 \approx 17$ fs. Since the energy required for this shift comes from the blue part of the spectrum, the entire spectrum shifts toward longer wavelengths. As expected, no NSR peak appears for $\delta_3=0$. Indeed, a distinct NSR peak appears only when δ_3 exceeds 0.015, again in agreement with the analytical results shown in Fig. 1. When $\delta_3=0.02$, the NSR peak occurs near $(\nu-\nu_s)T_0=4.5$ and it moves toward the central spectral region with increasing δ_3, as dictated by the phase-matching condition in Eq. (5). Note also that the peak amplitude is quite different when the IPRS effects are included,
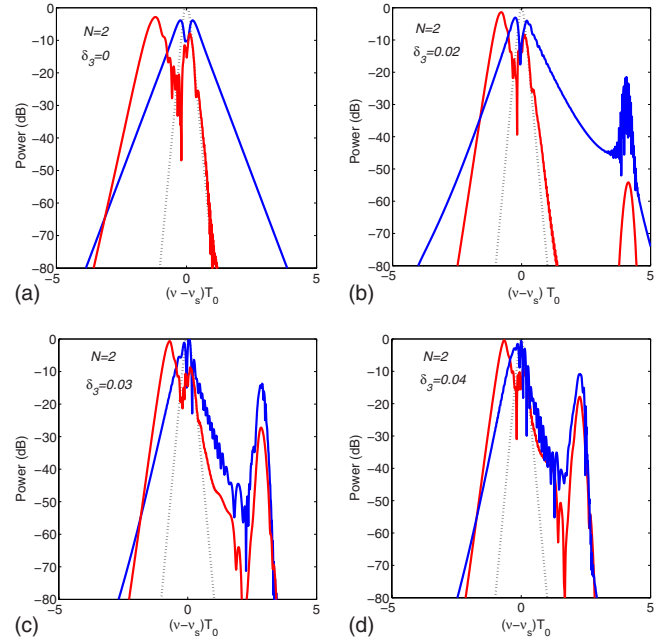
FIG. 2. (Color online) Output spectra at a distance of $4L_D$ for four values of δ_3 when a second-order soliton is launched into the fiber and all nonlinear effects are included (red solid curves). The dotted curve shows the spectrum of the input pulse. The darker (blue) curves show the spectrum when higher-order nonlinear effects are ignored.

indicating clearly that the higher-order nonlinear effects must be included for a quantitative understanding of any experimental data. The NSR-peak amplitude is always reduced by IPRS, and this reduction can be quite dramatic for relatively low values of δ_3, as is evident in Fig. 2(b) where peak power levels differ by more than 25 dB when δ_3 equals 0.02.

Another important noteworthy feature in Fig. 2 is that, not only is the NSR generated on the blue side for $\delta_3>0$, but other parts of the pulse spectrum are also affected by the presence of TOD. The shortest fundamental soliton, which shifts the most toward the red side because of IPRS, is affected the most by TOD. In particular, the magnitude of the redshift is reduced as δ_3 increases. Physically, this can be understood by noting that the energy loss of the soliton through NSR manifests as broadening of the Raman soliton. Since the IPRS-induced redshift scales inversely with the soliton width (as T_s^{-4}), any soliton broadening results in a reduced redshift.

IV. DEPENDENCE OF NSR ON THE TOD PARAMETER

As mentioned earlier, one of our objectives is to study systematically how the amplitude and frequency of the NSR change with changes in N and δ_3. We note from Fig. 2 that the normalized TOD parameter δ_3 plays a crucial role in controlling the NSR generation. Being dimensionless, one can get the same value of δ_3 for many different combinations of β_2, β_3, and T_0. Our results indicate that the resulting spectrum will be the same in all cases as long as δ_3 and N have the same values. With this feature in mind, we study numeri-
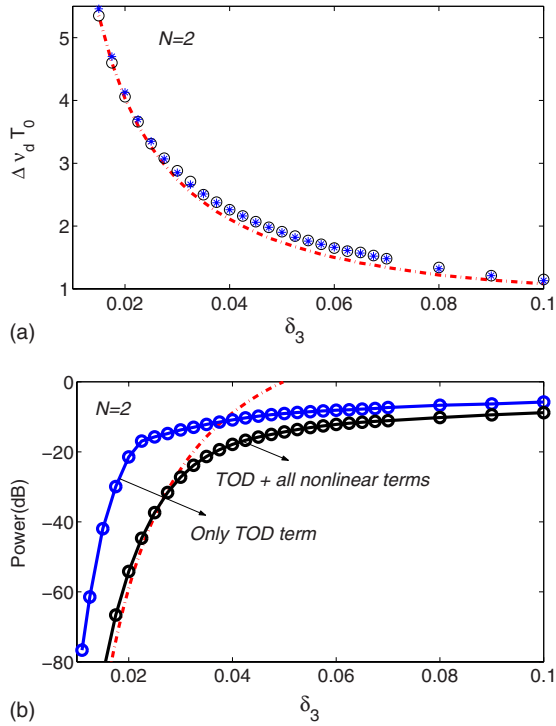
FIG. 3. (Color online) (a) Frequency shift and (b) relative peak power of the NSR peak plotted as a function of δ_3 (circles) and estimated from the numerically calculated output spectra similar to those shown in Fig. 2. Dot-dashed lines show the analytical prediction based on theory in Sec. II. The star symbols in (a) show the results obtained when higher-order nonlinear effects are neglected.

cally in this section how the amplitude and the frequency of the NSR peak vary with δ_3 for a given soliton order N. In particular, we focus on the $N=2$ case; larger values of N are considered in the next section.

An interesting question is how much the NSR amplitude and frequency are affected by the IPRS-induced redshift of the shortest soliton created through the fission process. Figure 3(a) shows the frequency and Fig. 3(b) the relative power of the NSR peak as a function of δ_3 for the second-order soliton ($N=2$) with (circles) and without (stars) the higher-order nonlinear effects included. Although the frequency of the NSR peak is not affected much by the IPRS, the amplitude of this peak is reduced significantly because of IPRS, especially for low values of δ_3 for which this reduction may exceed a factor of 20 dB. The continuous transfer of energy initiated by IPRS toward longer wavelengths may be responsible for this feature. Note that the amplitude of the dispersive wave first increases rapidly with increasing δ_3 (up to $\delta_3=0.04$ approximately) but then saturates for values of δ_3 > 0.05. Note also that it becomes difficult to separate the NSR peak from the rest of the pulse spectrum when δ_3 exceeds 0.1 because of the inverse dependence of $\Delta\nu_d$ on δ_3.

The important question is how well the approximate analytic predictions of Sec. II agree with our numerical results. The dot-dashed lines in Fig. 3 show the analytical prediction based on Eqs. (5) and (6). The numerical results for the NSR frequency in Fig. 3(a) agree well with this prediction for low values of δ_3. The agreement is reasonable even for higher

values of δ_3, even though the numerical values are consistently larger by about 5% or so. What is surprising is that the NSR frequency does not change much when IPRS is included. One possible explanation is that the NSR peak is generated right after the soliton fission. At that point, IPRS has not yet produced any spectral changes, and the prediction of Eq. (5) applies. Even though IPRS continuously shifts the soliton frequency toward the red side beyond this point, and the value of δ_3 changes because of changes in β_2 and β_3, it appears that these changes have no impact on the NSR frequency.

The situation is quite different as far as the amplitude of the NSR peak is concerned. The dashed line in Fig. 3(b) falls quite close to the numerical results obtained with the full NLSE that includes the higher-order nonlinear effects, but it deviates considerably from the data obtained in the absence of IPRS. In deriving Eq. (6), we used the peak power and pulse width of the shortest soliton, generated by the fission process and shifting the most toward the red side because of IPRS. The results show that our approximate analytic results given in Eqs. (5) and (6) can be used to predict the frequency and amplitude of the NSR peak under realistic conditions, as long as δ_3 is not too large, because the analytic results are valid only for relatively small values of δ_3 because of their perturbative nature. This is especially true in the case of the NSR amplitude. As seen in Fig. 3(b), the relative power of the NSR peak saturates to a value close to 10% of the input peak power. This is what one would expect on physical grounds.

V. DEPENDENCE OF NSR ON THE SOLITON ORDER

In this section we study how the frequency and amplitude of the NSR peak evolves with the soliton order N or, equivalently, with the input peak power [10]. The open circles in Fig. 4 mark the numerical values of these two quantities and the dashed line shows the analytic predictions. Consider first the case of the NSR amplitude shown in Fig. 4(b). For a fixed value of δ_3, this amplitude increases rapidly and then saturates to a value below 10% of the input peak power, a feature similar to that seen in Fig. 3(b). The analytical prediction agrees well with numerical simulation for $\delta_3=0.02$. The agreement is reasonable for $\delta_3=0.03$ as well for up to $N=3$, but large deviations occur for larger values of N. The reason is related to the perturbative nature of Eq. (6), which is valid as long as $(2N-1)\delta_3$ remains much less than 1. Our results show that large deviations occur when this quantity exceeds 0.15. This is precisely what one would expect. Our study also reveals that the IPRS reduces the NSR amplitude noticeably. The continuous shift of the Raman soliton toward longer wavelengths may be responsible for this behavior.

We next focus on the dependence of the frequency shift with the soliton order N shown in Fig. 4(a). As expected from theory of Sec. II, this frequency shift increases with increasing power. However, the agreement between the prediction of Eq. (5) and numerical data holds only for low values of N, and significant deviations between the two occur when N exceeds 3. The reason is again related to the perturbative nature of Eq. (5), which is valid as long as
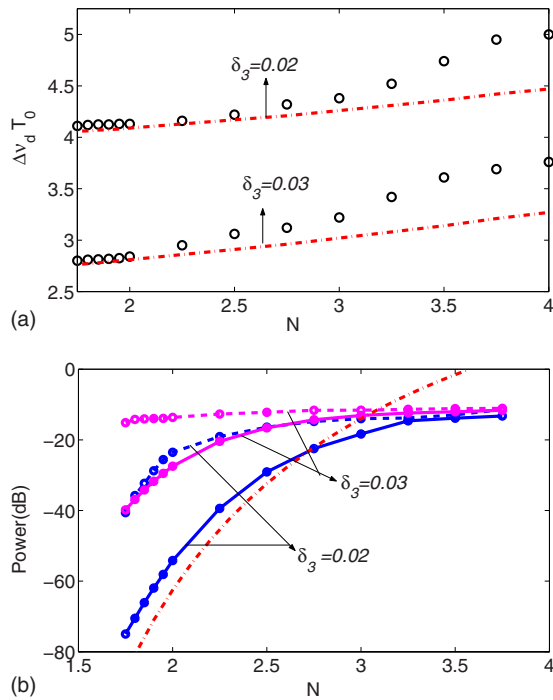
FIG. 4. (Color online) (a) Frequency shift and (b) relative peak power of the NSR peak plotted as a function of N (circles) and estimated from numerically calculated output spectra similar to those shown in Fig. 2. Dot-dashed lines show the analytical prediction based on theory in Sec. II. The black curves in part (b) show the results obtained when higher-order nonlinear effects are neglected.

$\varepsilon = (2N-1)\delta_3$ remains much less than 1. This quantity equals $5\delta_3$ when $N=3$ and exceeds $\varepsilon = 0.15$ for $\delta_3 = 0.03$. Clearly, we cannot expect the perturbation theory to hold for such a large value of the perturbation parameter. It is possible to calculate the NSR frequency more accurately. Indeed, the dashed curve in Fig. 4(a) was obtained by using a cubic polynomial [17] of the form $2\varepsilon x^3 + x^2 + 1 = 0$, where $x = \Delta\nu_d T_s$, from which Eq. (5) is derived to first order in ε after using the relation $T_s = T_0/(2N-1)$. However, the agreement remains poor for $N > 3$ even with this more accurate prediction. This is surprising and requires further study.

VI. CONCLUSIONS

Our work has focused on a realistic situation in which optical pulses are propagated as higher-order solitons inside optical fibers to generate a supercontinuum, and we thus include not only the TOD effects but two other nonlinear effects, namely, the IPRS and self-steepening, all of which perturb the solitons as they propagate down the fiber. Our main objective was to study how the NSR, emitted by the shortest fundamental soliton created after the fission process, is affected by TOD, IPRS, and the order N of the launched soliton. We were able to extend the perturbation analysis of Akhmediev and Karlsson [17] to the case of higher-order solitons and to find analytic expressions for the frequency and amplitude of the NSR peak that is generated in the output spectrum when a higher-order soliton is perturbed by the TOD.

We performed extensive numerical simulations to test how well the analytic predictions hold in practice. For this purpose, we employed a generalized NLSE written in terms of standard soliton units. This approach has the advantage of showing that the critical TOD parameter is not β_3 itself but a scaled dimensionless version of it, defined as $\delta_3 = \beta_3/(6\beta_2 T_0)$. Our results show that a certain minimum value of this dimensionless parameter is needed before the amplitude of the NSR peak becomes large enough that this peak is apparent in the output spectrum. This minimum value is about $\delta_3 = 0.06$ for fundamental solitons but it reduces to near 0.018 for second-order solitons ($N=2$) and falls below 0.1 for $N=3$. The amplitude of the NSR peak increases rapidly with both δ_3 and N but then saturates to a relative power level that is typically below 10% of the launched power. These results should be of relevance for applications in which a supercontinuum source is required.

[1] A. Hasegawa and M. Matsumoto, *Optical Solitons in Fibers* (Springer, New York, 2002).

[2] Yu. S. Kivshar and G. P. Agrawal, *Optical Solitons: From Fibers to Photonic Crystals* (Academic, Boston, 2003).

[3] J. P. Gordon and L. F. Mollenauer, *Solitons in Optical Fibers, Fundamentals and Applications* (Academic, Boston, 2006).

[4] G. P. Agrawal, *Nonlinear Fiber Optics*, 4th ed. (Academic, Boston, 2007).

[5] K. Tai, A. Hasegawa, and N. Bekki, Opt. Lett. **13**, 392 (1988).

[6] J. P. Gordon, Opt. Lett. **11**, 662 (1986).

[7] P. K. A. Wai, C. R. Menyuk, Y. C. Lee, and H. H. Chen, Opt. Lett. **11**, 464 (1986).

[8] J. M. Dudley, G. Genty, and S. Coen, Rev. Mod. Phys. **78**, 1135 (2006).

[9] A. V. Husakou and J. Herrmann, Phys. Rev. Lett. **87**, 203901 (2001).

[10] K. M. Hilligsøe, H. N. Paulsen, J. Thøgersen, S. R. Keiding, and J. J. Larsen, J. Opt. Soc. Am. B **20**, 1887 (2003).

[11] I. Cristiani, R. Tediosi, L. Tartara, and V. Degiorgio, Opt. Express **12**, 124 (2004).

[12] D. R. Austin, C. M. Sterke, B. J. Eggleton, and T. G. Brown, Opt. Express **14**, 11997 (2006).

[13] P. K. A. Wai, H. H. Chen, and Y. C. Lee, Phys. Rev. A **41**, 426 (1990).

[14] J. N. Elgin, Phys. Rev. A **47**, 4331 (1993).

[15] V. I. Karpman, Phys. Rev. E **47**, 2073 (1993).

[16] Y. Kodama, M. Romagnoli, S. Wabnitz, and M. Midrio, Opt. Lett. **19**, 165 (1994).

[17] N. Akhmediev and M. Karlsson, Phys. Rev. A **51**, 2602 (1995).

[18] J. N. Elgin, T. Brabec, and S. M. J. Kelly, Opt. Commun. **114**, 321 (1995).

[19] Q. Lin and G. P. Agrawal, Opt. Lett. **31**, 3086 (2006).